Springer

KSME

Journal of Mechanical Science and Technology 29 (2) (2015) 785~792
www.springerlink.com/content/1738-494x
DOI 10.1007/s12206-015-0140-z

Theoretical and experimental investigation of wear characteristics of aluminum based metal matrix composites using RSM †

S. Selvi[1,*] and E. Rajasekar[2]

[1]*Faculty of Mechanical Engineering, Institute of Road and Transport Technology, Erode – 638 316, Tamil Nadu, India*
[2]*Faculty of Automobile Engineering, Institute of Road and Transport Technology, Erode – 638 316, Tamil Nadu, India*

(Manuscript Received June 19, 2014; Revised October 31, 2014; Accepted November 13, 2014)

Abstract

The tribological properties such as wear rate, hardness of the aluminum-fly ash composite synthesized by stir casting were investigated by varying the weight % of fly ash from 5 to 20 with constant weight % of zinc and magnesium metal powder. A mathematical model was developed to predict the wear rate of aluminum metal matrix composites and the adequacy of the model was verified using analysis of variance. Scanning electron microscopy was used for the microstructure analysis which showed a uniform distribution of fly ash in the metal matrix. Energy - dispersive X-ray spectroscopy was used for the elemental analysis or chemical characterization of a sample. The results showed that addition of fly ash to aluminum based metal matrix improved both the mechanical and tribological properties of the composites. The fly ash particles improved the wear resistance of the metal matrix composites because the hardness of the samples taken increased as the fly ash content was increased.

Keywords: Dry sliding wear; Fly ash; Mathematical modeling; Metal matrix composite; Response surface methodology (RSM)

1. Introduction

In the recent past, a new class of material, quite particularly metal matrix composites, is becoming more and more important as it plays a vital role in the advanced material science and materials engineering. Aluminum and its alloys are highly useful in automobile, aerospace, marine and medical applications because of their low density, high specific strength, dimensional stability, corrosion resistance and high thermal conductivity. Conventional Al alloys exhibit poor tribological properties. Addition of fly ash or ceramic particulates with little percentage of zinc and magnesium results in better properties.

The mechanical properties of the MMCs mainly depend on the type, size, shape, volume fraction and special distribution of fly ash and magnesium particles in the aluminum matrix [1]. MMCs are fabricated by powder metallurgy, stir casting, mechanical alloying etc. [2]. Rajan et al. [3] investigated the properties of Al-Si-fly ash composite characteristics by stir casting routes. Babu Rao et al. [4] found that stir casting is more simple and suitable for large quantity fabrication. Hence, in this work, stir casting method is employed for MMC fabrication using different composition of reinforcing materials. Ramachandra and Radhakrishna [5] observed a significant increase in wear resistance and that hardness can be conferred with small reinforcement volume fraction.

2. Matrix and reinforcement materials

2.1 Materials and MMC preparation

The matrix metal used in this investigation is commercial aluminum with a purity of 98.5% and the main reinforcement material is fly ash particulates with an average particle size of 10-30 μm and its chemical composition is listed in Table 1. Majority of fly ash contain silica, alumina, calcium sulphate and un-burnt carbon in them. The fly ash shown in Fig. 1 was collected from Neyveli Lignite Corporation, Tamil Nadu, India. 500 g of fly ash was preheated at about 750˚C for 3 hours and the loss of ignition was found to be 2.23% and then it was cooled to atmospheric temperature.

2.2 Wear characterization on Al – fly ash composite

Tribological properties studied by Ramachandra and Radhakrishna [6] on Al-Si-fly ash revealed that the wear rate decreased linearly as the volume fraction of Si and fly ash increased. Deuis et al. [7] showed that Al-Si alloys and Al based MMCs containing hard particles offer superior operating performance and resistance to wear and hence a longer service

*Corresponding author. Tel.: +91 04242533279, Fax.: +91 04242533590
E-mail address: selvimech@yahoo.com
† Recommended by Associate Editor In-Ha Sung

Table 1. Chemical composition of fly ash in wt %.

SiO_2	Al_2O_3	Fe_2O_3	TiO_2	CaO	MgO	Na_2O	K_2O	Loss on ignition
59.04	30.02	8.75	2.46	1.0	1.01	0.99	1.89	2.23

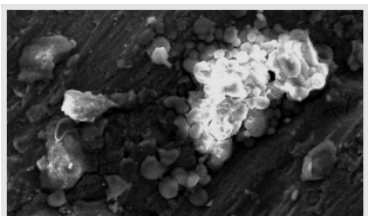

Fig. 1. SEM micrograph of fly ash used.

life. The study by Sannino and Rack [8] showed that the aluminum composites resulted in high wear resistance due to increased fly ash content. Samrat Mohanty and Chugh [9] developed the automotive brake lining by adding fly ash with Al and showed that formulated brakes test samples, outperformed the commercially available original brake pads. De Mello [10] reported that SiC reinforcement with Al increased the abrasion resistance to an appreciable level.

3. Sample preparation

The synthesis of Al MMC used in this study was carried out by stir casting technique. Al in the form of circular rods and the reinforcement materials in the form of particulates were used for trials. Initially, the furnace temperature was maintained at 725°C while melting the aluminum rods. With progressive melting, temperature was raised to 800°C, and then 0.5% Mg to increase the wettability of the fly ash particles and 0.1% of Zn powder was added to the molten metal and held at this temperature for 30 minutes and a vortex motion was created using a graphite stirrer. When the stirring was continued, fly ash, Zn and Mg were introduced at a uniform rate. The molten Al was stirred at 250 rpm by using argon as shielding gas and stirring was continued for 20 minutes after the addition of fly ash in order to get a thorough mixing and uniform distribution in the molten metal. The molt was allowed to solidify and the castings were obtained with different mass fractions of fly ash. The specimens were polished and etched and all the specimens were cut and tested.

3.1 Mechanical and metallurgical characterization on Al MMCs

Specimens for metallographic observations were sectioned from the as cast non reinforced aluminum and reinforced composites. The cut samples were mechanically grounded by initial rough grinding using SiC impregnated emery paper of grit size 200-300 and fine grinding with grit size 600-700 and then the grounded samples were polished by 1μm aluminum powder. Etching of polished samples was done using Keller's reagent [11]. Scanning electron microscope was used to evaluate the morphological changes occurring in the composites. Energy-dispersive X-ray spectroscopy was used in this study for the chemical characterization of the samples.

Table 2. Sliding wear parameters and their levels.

Parameters	Notations	Unit	Levels				
			-2	-1	0	1	2
Sliding distance	D	m	1000	1500	2000	2500	3000
Speed	N	rpm	400	800	1200	1600	2000
Load	F	N	29.4	49.1	68.7	88.3	107.9
Fly ash	c	%	0	5	10	15	20

3.2 Hardness test

The hardness of pure Al and composites were determined using Rockwell hardness testing machine. The test was conducted on each specimen with 100 kg load and a 1.587 mm steel ball intender. The detention time for the hardness measurement was 20 seconds [12].

3.3 Wear characterization analysis by dry sliding wear test

To analyze the wear properties of Al MMCs, computerized DUCOM pin-on-disc sliding wear testing machine was used and the tests were carried out as per ASTM G99-05 standards [13]. Dry sliding wear behavior of the Al MMCs was investigated by varying applied normal load, % fly ash content variation, sliding distance and sliding velocity. The wear loss on the specimen was recorded during each test and the volume loss due to wear was calculated for each specimen. Each trial was repeated twice and the average volume loss was taken for the analysis of wear behavior.

4. Development of mathematical model for wear rate

Response surface methodology is one of the most informative methods of analysis of the result of a factorial experiment. The sliding wear parameters and their levels are shown in Table 2. The response wear rate 'W' is expressed as a function of process parameters sliding distance (D), speed (N), load (F) and mass fraction of fly ash content (c),

$$W = f(D, N, F, c) . \quad (1)$$

When the mathematical form of 'f' is unknown, this function can be approximated within the experimental region by polynomials in terms of process parameter variable. Box and Hunter proposed central composite rotatable design for fitting a second order response surface based on the criterion of rotatability [14]. The central composite rotatable factorial design consisting of 32 sets of coded conditions shown in Table 3 was used to carry out the experiments. The design for the

Table 3. Experimental design matrix.

Trial run	Sliding wear parameters				
	D	N	F	c	Wear rate (10^{-5} mm^3m^{-1})
T01	-1	-1	-1	-1	510
T02	1	-1	-1	-1	545
T03	-1	1	-1	-1	537
T04	1	1	-1	-1	593
T05	-1	-1	1	-1	535
T06	1	-1	1	-1	589
T07	-1	1	1	-1	560
T08	1	1	1	-1	628
T09	-1	-1	-1	1	330
T10	1	-1	-1	1	355
T11	-1	1	-1	1	365
T12	1	1	-1	1	383
T13	-1	-1	1	1	351
T14	1	-1	1	1	375
T15	-1	1	1	1	387
T16	1	1	1	1	428
T17	-2	0	0	0	396
T18	2	0	0	0	520
T19	0	-2	0	0	395
T20	0	2	0	0	505
T21	0	0	-2	0	403
T22	0	0	2	0	514
T23	0	0	0	-2	710
T24	0	0	0	2	295
T25	0	0	0	0	446
T26	0	0	0	0	457
T27	0	0	0	0	451
T28	0	0	0	0	432
T29	0	0	0	0	453
T30	0	0	0	0	452
T31	0	0	0	0	448
T32	0	0	0	0	441

above experiment comprises of a half replication of 2^5 factorial design plus 7 center points and 8 star points. These correspond to first 16 rows, the last 6 rows and rows from 17 to 26 respectively in the design matrix shown. For half replicate the extra point included to form a central composite design, α becomes $2^{(k-1)/4} = 2$. The intermediate values are coded as -1, 0 and +1. The upper and the lower limit of the parameter is coded as +2, and -2 and the coded values for the intermediate values are calculated by using the relationship [15]

$$X_i = \frac{2\left[2X - \left(X_{max} + X_{min}\right)\right]}{\left[X_{max} - X_{min}\right]}. \quad (2)$$

The second order polynomial regression equation used to represent the response surface '*Y*' for k factors [16] is given by

$$Y = b_0 + \sum_{i=1}^{k} b_i X_i + \sum_{i=1}^{k} b_{ii} X_i^2 + \sum_{i=1}^{k} b_{ij} X_i X_j \quad (3)$$

where b_0 is the average of responses, and b_i, b_{ii} and b_{ij} are the coefficients which depend on the respective main and interaction effects of the parameters [17]. The statistical software SYSTAT 13 was used to determine the coefficients. The selected polynomial for the four factors is represented as follows:

$$W = b_0+b_1D+b_2N+b_3F+b_4c+b_{11}D^2+b_{22}N^2+b_{33}F^2+b_{44}c^2+ b_{12}DN+b_{13}DF+b_{14}Dc+b_{23}NF+b_{24}Nc+b_{34}Fc\,. \quad (4)$$

The mathematical model was developed after determining the essential coefficients and tested for their significance at 95% confidence level as done by Ref. [18]. The developed final mathematical model with dry sliding wear parameters in coded form is given as:

$$W = 452.763+23.708D+21.292N+19.042F- 98.042c+13.014c^2. \quad (5)$$

Table 4. Adequacy of ANOVA test results of the developed model.

Dependant variable	Wear rate
N	31
Squared multiple R	0.958
Adjusted squared multiple R	0.944
Standard error of estimate	0.0003769

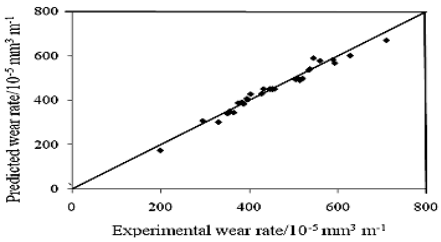

Fig. 2. Scatter diagram for developed model.

4.1 Verification of the adequacy of the model

Table 4 clearly indicates the adequacy test results of the mathematical model. R^2 value is 0.958, which shows that 95.8% of the experimental data fits into the developed model. The model has given an error value of 0.0003769, which is indicated as standard error of estimate and these values confirm the significance of the individual parameters.

Fig. 2 shows that the experimental values and predicted values from the mathematical model are scattered on both sides and close to 45° line, which further proves the adequacy of the model.

The predicted wear rate was calculated using the equation (5) and the relationship between the experimental wear rate and predicted wear rate with respect to the trail runs carried out is plotted in Fig. 3 and it is found that the experimental and the predicted values are much closer to each other and a little deviation is observed.

4.2 Confirmation of the experiment

In order to validate the regression model, confirmation wear

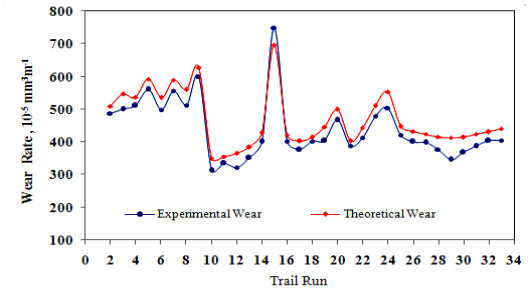

Fig. 3. Theoretical and experimental wear rate.

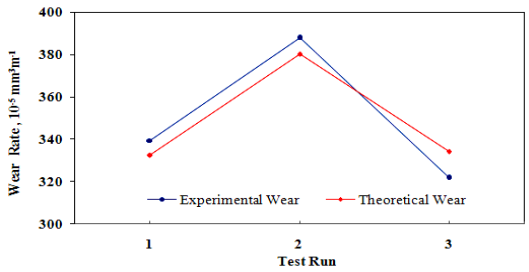

Fig. 4. Confirmation test results.

tests were conducted with parameter levels that were different from those for analysis. The results were plotted in Fig. 4 and the deviation is found to be minimum.

5. Results and discussions

5.1 Effect of fly ash reinforcement on hardness

Fig. 5 shows the hardness of the Al composites as a function of mass fraction of fly ash content in as cast condition. The hardness observed for Al was 27 HRc and 40 HRc for 20 wt% reinforced Al MMC. The increase in fly ash content improves the hardness of the composite, due to the presence of more silica and alumina which are generally hard in nature in the fly ash [19]. Also, a slight variation was found in the hardness of Al with 15 and 20 wt% of fly ash and noted that further increase of fly ash particles do not have any effect on hardness.

5.2 Effect of content of fly ash on wear rate

Fig. 6 shows the wear rate of the composites as a function of volume fraction of fly ash content at a normal load of 68.7 N. The wear rate gradually decreased with increase in fly ash content. This is mainly due to the presence of hard silica particles in the fly ash.

5.3 Effect of hardness on wear rate

The effect of hardness on the wear rate is indicated in Fig. 7. As the hardness increases, the wear rate decreases appreciably to a minimum value, mainly due to increase of the reinforcement material. The presence of fly ash particles will increase

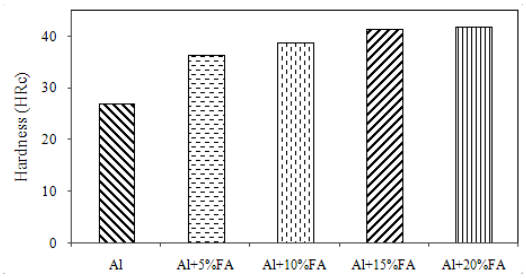

Fig. 5. Effect of fly ash addition on hardness of Al fly ash composites.

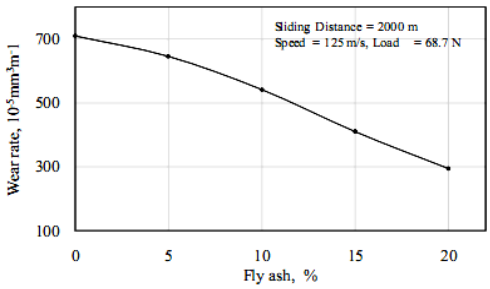

Fig. 6. Effect of fly ash content on wear rate.

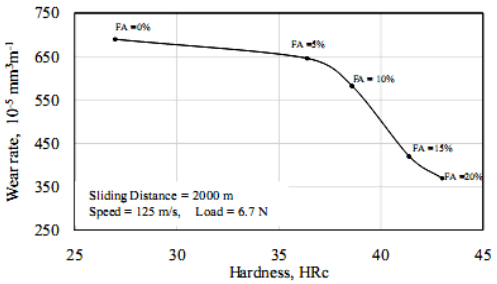

Fig. 7. Effect of hardness on wear rate.

the overall bulk hardness of the composite material and hence the decrease in wear rate is observed.

5.4 Effect of normal load on wear rate

The dry sliding wear tests conducted on the five samples revealed that the load was one of the main parameters influencing the wear rate of the composites. It is observed from the Fig. 8, as the applied load increased, the wear rate also increased. The predominant factor for this behavior was found to be adhesive wear. The increase in applied load increases the coefficient of friction which causes high wear rate. This will result in undesirable effects like micro-ploughing, delamination etc. [20].

5.5 Effect of sliding velocity on wear rate

From Fig. 9, it is evident that the increase in sliding velocity increases the wear rate. Increase in speed causes the plastic deformation on wear surfaces and sub surfaces.

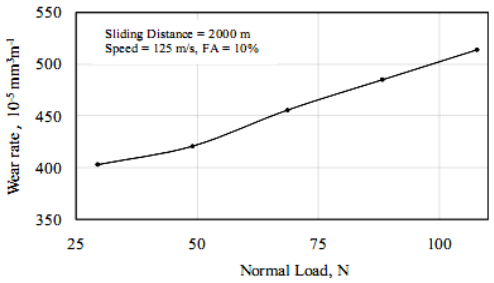

Fig. 8. Effect of applied normal load on wear rate.

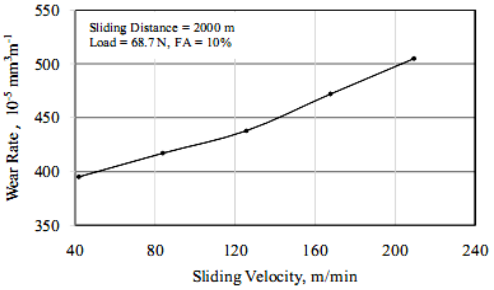

Fig. 9. Effect of sliding velocity on wear rate.

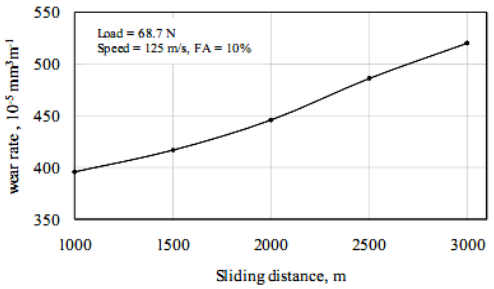

Fig. 10. Effect of sliding distance on wear rate.

At higher sliding velocities, thermal softening takes place as the surface temperature rises. This results in severe wear rate. High sliding velocities result in surface frictional heating, which in turn results in the formation of a thin molten layer at asperity contacts.

5.6 Effect of sliding distance on wear rate

Fig. 10 depicts the direct effect of sliding distance on wear rate. As the distance increases, more surfaces are exposed to wear process and the wear debris also increases thereby resulting in severe wear loss. In the mild wear regime, volume loss due to wear increased linearly with the sliding distance which indicates that wear progressed under the steady state conditions.

5.7 Effect of sliding time on wear rate

Fig. 11 shows the direct effect of sliding time on wear rate. It is clear from the figure that the wear rate is linearly increasing with the increase in sliding time. As the time increases, surfaces are exposed to high wear rate and the quantity of wear debris also increases thereby resulting in severe wear loss.

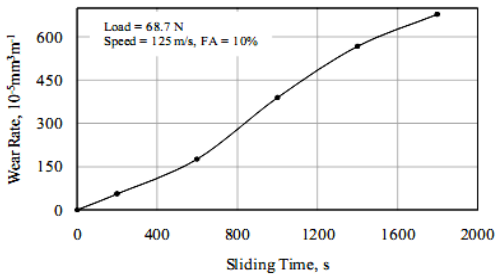

Fig. 11. Effect of sliding time on wear rate.

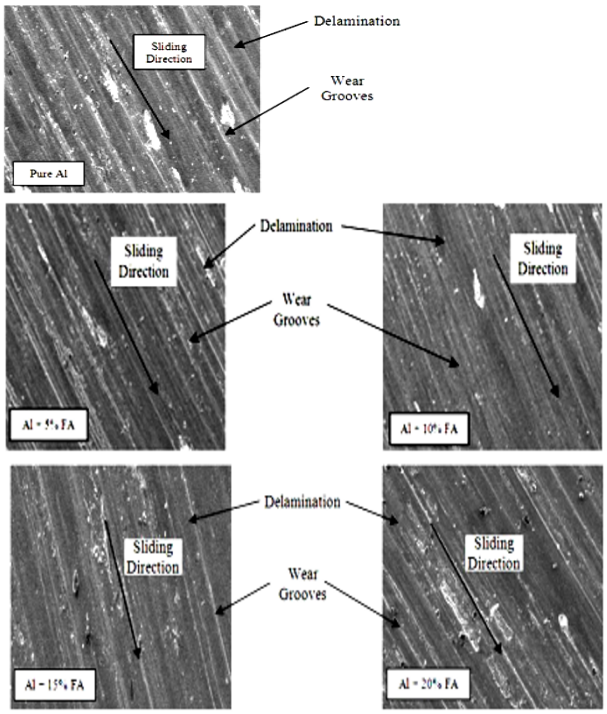

Fig. 12. SEM micrograph of Al - fly ash composites.

5.8 SEM and EDAX analysis of Al MMCs

To understand the morphologies and chemical composition of the Al and Al MMC, SEM microstructure analysis and EDAX were carried out. Number of grooves, parallel to the sliding direction, is evident on all the samples which are shown in Fig. 12. This was mainly due to abrasion at high load. Good retention of fly ash particles was clearly observed in the microstructures of Al MMC [21]. Also delamination was observed in the samples, which leads to separation of layers of reinforcement or plies [22, 23].

EDAX is used to confirm the interactions between the fly ash particles and the metal matrix. The results of EDAX

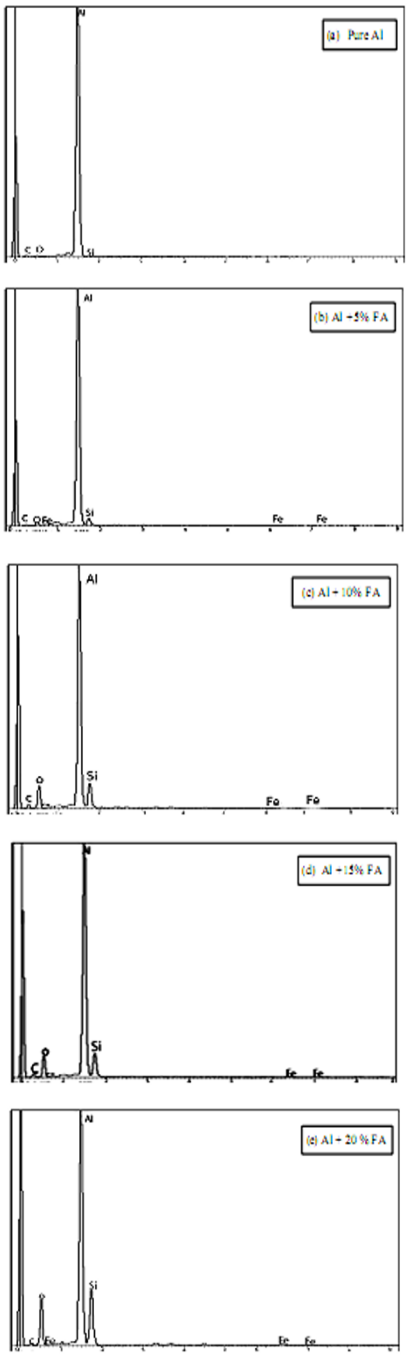

Fig. 13. EDAX spectrum showing the presence of Al, Si, O, C & Fe (Increase in Si shows the increase in fly ash content added in MMC).

analysis are shown in Fig. 13. Fig. 13(a) indicates the results for pure Al with very little traces of SiC and oxides.

Figs. 13(b)-(e) depict the results of EDAX for Al with 5, 10,15 and 20 wt% fly ash content respectively, where a small increase in the values of Si and oxides was noted. Fig. 13(d) shows the results for 15% fly ash content, which showed comparatively a greater increase in Si and oxides [24]. A predominant increase of the same elements was observed for 20% fly ash content which is shown in Fig. 13(e).

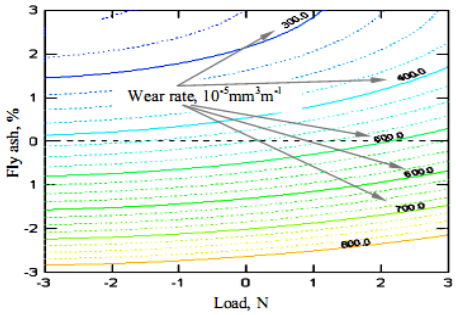

Fig. 14. Contour plot of wear rate vs load & fly ash %.

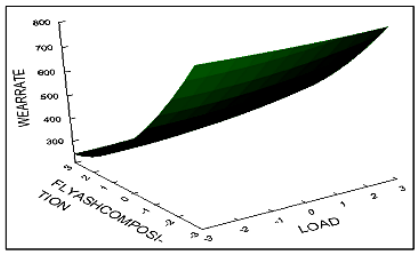

Fig. 15. Surface plot of wear rate vs load & fly ash %.

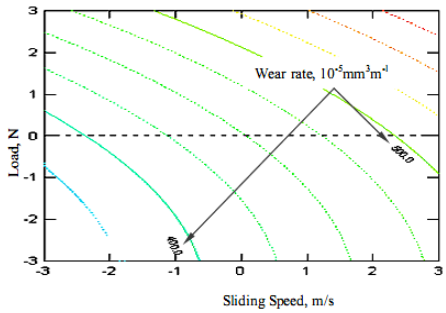

Fig. 16. Contour plot of wear rate vs load & sliding speed.

6. Response surface for interaction effect of variables

6.1 Interaction effect of load and fly ash composition on the wear rate

Fig. 14 shows the interaction effect of load and volume fraction of fly ash reinforcement on the wear rate which clearly reveals that the wear rate decreases with increase in % fly ash particulates. Also it is found that increase in applied load increases the wear rate. Maximum wear rate of 800 x 10^{-5} mm^3m^{-1} was observed at maximum load (+2) of 107.91 N and minimum fly ash content (level -3). Similarly the results can be compared for other levels of load and fly ash content. The reinforcement of fly ash offers a minimum wear rate. The same trend is indicated in the surface plot as shown in Fig. 15.

6.2 Interaction effect of load and sliding speed on the wear rate

Figs. 16 and 17 indicate the effect of speed and load on the wear rate.

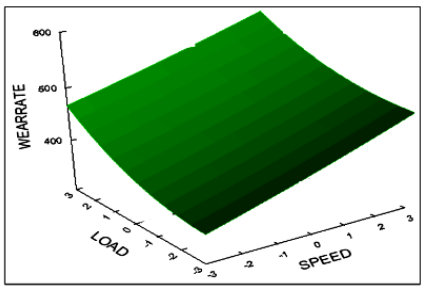

Fig. 17. Surface plot of wear rate vs load & sliding speed.

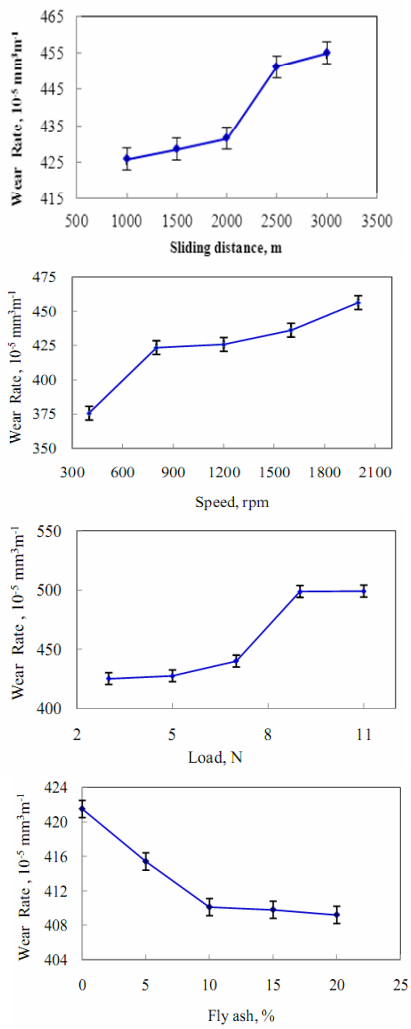

Fig. 18. ANOVA interaction graphs.

As the load and speed increases from lower level (-3) to higher level (+3) the wear rate also increases. This may be due to quick plastic deformation of material at the surfaces and sub-surfaces when it is subjected to a severe dry sliding wear.

6.3 Interaction effect of design parameters on ANOVA

Fig. 18 shows the error band for the design parameters sliding distance, speed, load and fly ash percentage. These results are plotted from the least square values obtained from ANOVA. It is clear from the figures, that the design is significant since the error values are within the permissible limit.

7. Conclusions

The following conclusions were arrived as a result of the present study on the wear behavior of Al MMC samples processed by stir cast method:

- The investigation presented a central composite rotatable second order response surface methodology to develop a mathematical model to predict the wear rate of Al MMCs in terms of fly ash composition, applied normal load and sliding speed.
- It was clear from the mathematical model that the wear loss increased with normal load. But wear rate decreased as the fly ash content increased.
- Defect free aluminum matrix fly ash reinforced composite was produced by a more economical and simple stir casting method.
- The hardness of the Al MMCs increased as the fly ash content increased.
- The presence of SiO_2 in fly ash improved the wear resistance of Al MMC to an appreciable limit and the results have good agreement with other studies.
- SEM microstructure of composites reveals the uniform distribution of fly ash particulates in the metal matrix.

Nomenclature

X_i : Required coded value of the variable X

X : Any value of the variable from X_{max} to X_{min}

X_{max} & X_{min} : Upper & Lower limit of the variable

References

[1] I. Dinaharan, N. Murugan and S. Parameshwaran, Influence of in-situ formed ZrB_2 particles on microstructure and mechanical properties of AA6061 metal matrix composite, *Material Science and Engineering* A, 528 (2011) 5733.

[2] J. B. Fogagnolo, M. H. Robert, E. M. R. Navas and J. M. Torralba, *6061* Al reinforced with zirconium diboride particles processed by conventional powder metallurgy and mechanical alloying, *Materials Science,* 39 (2004) 127.

[3] T. P. D. Rajan, R. M. Pillai, B. C. Pai, K. G. Sathyanarayana and P. K. Rohatgi, Fabrication and characterization of Al-7Si-0.35Mg/fly ash metal matrix composites processed by different stir casting route, *Composites Science and Technology,* 67 (2007) 3369.

[4] J. Babu Rao, D. Venkat Rao and R. Bhargava, Development of light weight ALFA composites, *Engineering, Science and Technology,* 2 (11) (2010) 50.

[5] M. Ramachandra and K. Radhakrishna, Effect of reinforcement of fly ash on sliding wear, slurry erosive wear and cor-

rosive behavior of aluminum matrix composite, *Wear,* 262 (2007) 1450.
[6] M. Ramachandra and K. Radhakrishna, Synthesis-microstructure-mechanical properties -wear and corrosion behavior of Al-Si (12%) – Fly ash metal matrix composite, *Material Science,* 40 (2005) 5989.
[7] R. L. Deuis, C. Subramanian and J. M. Yellup, Abrasive wear of aluminum composites – a review, *Wear*, 201 (1996) 132.
[8] A. P. Sannino and H. J. Rack, Dry sliding wear of discontinuously reinforced aluminum composites: review & discussion, *Wear,* 245 (2000) 22.
[9] S. Mohanty and Y. P. Chugh, Development of fly ash- based automotive brake lining, *Tribology International,* 40 (2007) 1217.
[10] J. B. D. De Mello, Three-body abrasion of Al-Si composites, *Wear,* 225 (1999) 163.
[11] S. C. Tjong and Z. Y. Ma, Microstructural and mechanical characteristics of in - situ metal matrix composites, *Materials Science and Engineering,* 67 (2000) 3369.
[12] D. Tabor, *The hardness of metals* glasgow: Oxford University Press, UK (1951).
[13] G. Withers, Dispersing fly ash particles in an aluminum matrix, *Advanced Materials and Processes* (2006) 39.
[14] W. G. Cochran and G. M. Cox, *Experimental design*, Asia Publishing House, India (1963).
[15] D. G. Montgomery, *Design and analysis of experiments*, John Wiley and Sons, NY (2009).
[16] P. S. Sivasakthivel, V. Vel Murugan and R. Sudhakaran, Prediction of tool wear from machining parameters by response surface methodology in end milling, *Engineering Science and Technology,* 2 (6) (2010) 1780.
[17] H. Oktem, T. Erzurumlu and H. Huurtaran, Application of response surface methodology in the optimization of cutting conditions for surface roughness, *Materials Processing and Technology* (2005) 170.
[18] I. Dinaharan and N. Murugan, Dry sliding wear behavior of AA 6061 / ZrB_2 in - situ composite, *Transactions of Nonferrous Metals Society of China,* Elsevier, 22 (2012) 810.
[19] T. J. A. Doel, M. H. Loretto and P. Bowen, Mechanical properties of aluminum based particulate metal matrix composites, *Composites,* 24 (1993) 270.
[20] A. P. Sannino and H. J. Rack, Tribological investigation of Al-20 volume % SiCp/17-4 pH, *Part 1 Composite Performance, Wear,* 196 (1996) 202.
[21] H. Gletier, Nanostructured materials; Basic concept and microstructure, *Acta Materialia,* 48 (1) (2000).
[22] T. Rajmohan, K. Palaanikumar and S. Ranganathan, Evaluation of mechanical and wear properties of hybrid aluminium matrix composites, *Trans. Nonferrous Met.* Soc. China, 23 (2013) 2509.
[23] J. Zhang and A. T. Alpas, Delamination wear in ductile materials containing second phase particles, *Mater. Sci. Eng.* A, 160 (1993) 25.
[24] B. D. Cullity and S. R. Stock, *Elements of X-ray diffraction*, Upper Saddle River. NJ: Prentice Hall (2000).

S. Selvi graduated in 1992 with a degree in M.E. degree (with Distinction) from Anna University, Chennai. She obtained her Ph.D. in Mechanical Engineering in 2010 from Bharathiar University, Coimbatore. She has received the best paper award from Indian Institute of Welding (IIW) in 2008 and second best paper award from BHEL, WRI, Trichy in 2009. Currently she is an Associate Professor in Mechanical Engineering, IRTT, Erode. Her main research activities focus on metal matrix composites, welding and hardfacing.

E. Rajasekar completed his M.E. degree (with Distinction) in Automobile Engineering discipline in 1992 from Anna University, Chennai and Ph.D. in Mechanical Engineering in 2011 from Anna University, Chennai. He is an Associate Professor in Automobile Engineering, IRTT, Erode. He is an active member in the SAE India, Combustion Institute, Institution of Engineers (India) and ISTE. His research interest is mainly on automotive materials, alternative fuels for IC Engines and renewable energy.